Thermodynamic analysis of cycle arrangements of the coal-fired thermal power plants with carbon capture

VLADIMIR OLEGOVICH KINDRA[*]
IGOR ALEXANDROVICH MILUKOV
IGOR VLADIMIROVICH SHEVCHENKO
SOFIA IGOREVNA SHABALOVA
DMITRIY SERGEEVICH KOVALEV

National Research University "Moscow Power Engineering Institute", Krasnokazarmennaya 14, Moscow, 111250 Russia

Abstract The electricity production by combustion of organic fuels, es-pecially coal, increases the atmospheric CO_2 content, which contributes to global warming. The greenhouse gas emissions by the power production in-dustry may be reduced by the application of CO_2 capture and storage sys-tems, but it remarkably decreases the thermal power plant (TPP) efficiency because of the considerable increase of the auxiliary electricity requirements. This paper describes the thermodynamic analysis of a combined cycle TPP with coal gasification and preliminary carbon dioxide capture from the syn-gas. Utilization of the heat produced in the fuel preparation increases the TPP net efficiency from 42.3% to 47.2%. Moreover, the analysis included the combined cycle power plant with coal gasification and the CO_2 cap-ture from the heat recovery steam generator exhaust gas, and the oxy-fuel combustion power cycle with coal gasification. The coal-fired combined cy-cle power plant efficiency with the preliminary CO_2 capture from syngas is 0.6% higher than that of the CO_2 capture after combustion and 9.9% higher than that with the oxy-fuel combustion and further CO_2 capture. The spe-cific CO_2 emissions are equal to 103 g/kWh for the case of CO_2 capture from syngas, 90 g/kWh for the case of CO_2 capture from the exhaust gas and 9 g/kWh for the case of oxy-fuel combustion.

Keywords: Combined cycle power plant; Carbon capture and storage system; Pre-combustion capture; Post-combustion capture; Oxy-fuel combustion

Introduction

The carbon dioxide (CO_2) atmospheric content is about 410 ppm [1] and has grown by 10% in the last two decades [2]. The carbon dioxide leading producers are China, the USA, India, and Russia [3].

Nowadays reduction of greenhouse gases emission is one of the most important tasks. The 2015 Paris climate agreement requires carbon dioxide emissions to reach zero level by 2050 [4,5]. The world power industry mostly produces heat and electricity but its carbon dioxide emissions are about a quarter of the world amount [6]. It is proposed to reduce the power industry emissions by the introduction of renewable power sources, nuclear power plants, and low-carbon thermal power plant (TPP) technology.

Introduction of the renewable power sources is limited by the low density of energy flow and its irregularity. Nuclear power plant production is related to the risk of accidents that may cause radiation pollution. These factors and the wide use of TPP make prospects for carbon capture and storage (CCS) technology. On the other side, this technology has high power con-sumption and requires large operation and investment outlays. Thus, the wide CCS introduction requires searches for the most efficient and envi-ronmentally safe version of the TPP cycle arrangement that provides the required emission reduction combined with the acceptable fuel consumption and moderate cost.

The CCS concept may be presented in three directions (Fig. 1), the pre-combustion carbon dioxide capture, the post-combustion capture and the oxy-fuel combustion capture. Versions of these technologies provide an 85–99% capture degree [7, 8].

Each of the technology versions may be split into a few sub-technologies. The pre-combustion capture involves the absorption by physical or chemical reactants. In the physical absorption technology, the captured CO_2 price is 25–30 U.S. dollar per ton which is remarkably cheaper than the 40–50 U.S. dollar per ton in the chemical absorption [9], because after the CO_2 separa-
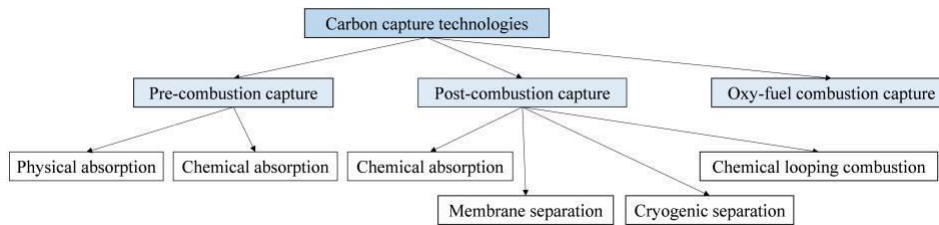
Figure 1: Carbon capture technologies.

tion the absorbent may be completely separated from the absorbate. In this technology, the syngas is preliminarily enriched where its hydrogen content in the fuel mixture is increased and the carbon monoxide is transformed into carbon dioxide. Then the CO_2 is separated by a physical absorbent and is supplied to the CCS [10, 11]. This technology may be used only in the pre-combustion capture when the gas fuel produced by the natural gas conversion or by gasification has a pressure above 8 bar [12].

The post-combustion technology may employ the membrane [13–15] or cryogenic [16,17] separation, or the oxy-fuel combustion capture [18–20], or the chemical looping combustion [21–24], or the chemical reagent absorp-tion like in the pre-combustion capture technology. These technologies may be used for modification of the existing steam turbine and combined cycle power plants, or the new TPP construction. Table 1 summarizes the main performance of the post-combustion carbon dioxide capture. It shows that the widely used CO_2 chemical absorption from exhaust gas is one of the most efficient methods.

Table 1: Comparison of the post-combustion carbon capture technology characteristics.

Parameter	Carbon capture technologies			
	Chemical absorption	Membrane separation	Cryogenic separation	Chemical looping combustion
Specific energy consumption for CO_2 capture, MJ/kg	0.59–2.83	0.6–6.0	0.49–3.4	3.8–4.9
CO_2 capture rate, %	85–90	80–90	> 95	> 95

The advantages of the carbon dioxide capture with monoethanol amine (MEA) are the high capture degree of 85–90% in a wide range of its par-tial pressures, the high chemical stability and the high reaction capability. The technology shortages are the absorbent losses that need a refill, the

surface's corrosion and the high price. Despite these shortages, the MEA capture technology is the best approved and relatively cheap, so it is widely used [25–29].

Another advanced direction to the CO_2 emission reduction is the transition to oxy-fuel combustion power cycles. The organic fuel combustion in the oxygen area produces a two-component working fluid which allows its split into carbon dioxide and water vapor through the vapor condensing [30]. In this method, the CO_2 capture degree is about 99%.

Numerous papers compare the influence of different capture systems upon the power plant efficiency. Specifically paper [12] discloses the thermal efficiency comparison results of a natural gas-fired combined cycle power plant equipped with the post-combustion CCS system with a coal-fired steam turbine power plant equipped with the CCS system and the coal-fired integrated gasification combined cycle (IGCC) equipped with the pre-combustion CCS system. The conclusion is that the most efficient coal-fired power production is reached in IGCC with the physical absorption of carbon dioxide. However, among the reviewed TPP versions there were neither coal-fired IGCC with the post-combustion carbon capture nor oxy-fuel combustion power cycle with the carbon dioxide working fluid. In turn, the paper [31] reviews all three methods in a combined cycle TPP with coal gasification and it mentions that oxy-fuel combustion requires new solutions in the power production equipment design. It is worth mentioning that the published papers don't compare the most efficient coal-fired TPP flow concepts with different CCS systems at currently available working fluid parameters. Therefore, in this paper the comparison is carried out for the most efficient versions of the coal-fired TPP with low greenhouse gases emission as the following:

- IGCC with pre-combustion capture with the CO_2 physical absorption separation from the coal gasification syngas;

- IGCC with post-combustion capture with the CO_2 chemical absorption from flue gas with the monomethanol amine solvent;

- oxy-fuel combustion power plant based on the Allam cycle that is one of the most efficient oxy-fuel combustion power cycles [20, 32, 33].

The additional thermodynamic analysis discloses the utilization of the heat produced in the syngas preparation before its firing in IGCC.

2   Research object

The combined cycle power plants with steam-oxygen coal gasification equip-ped with CCS systems are studied in this work. The power plants in this study differ by the CO_2 capture technology.

The first unit (Fig. 2a) is a coal-fired IGCC. Gasification block *3* trans-forms coal into syngas. It consists of the gasifier and the ash interception. The processing oxygen is produced by the air separation unit (ASU) *1* from the atmosphere air and compressed up to gasifier pressure in the inter-cooled oxygen compressor *2*. The processing steam is taken from the steam turbine *14*. Then the syngas is fired in the gas turbine combustion chamber *5*. The air compressor *4* compresses air. Some air is supplied to the gas turbine *6* cooling. The gas turbine *6* is mounted together with the power generator *7* on a single shaft. Then the gas turbine exhaust enters the double-pressure heat recovery steam generator (HRSG) where it transfers its heat to the steam turbine cycle through heat exchanger surfaces. Then the block *21* captures the exhaust gas CO_2 by the chemical absorption method. The CO_2 is compressed in compressor *22* and sent to its storage.

In the steam turbine cycle, downstream the condenser *16* the condensate pump *19* supplies water to the condensate gas heater *13*. Upstream the heater a part of the heated water is recirculated with the recirculation pump *20*. Then the water passes the deaerator *15* and is split into two the low- and high-pressure flows by the feedwater pumps *17* and *18*. The low-pressure feedwater sequentially passes the low-pressure vaporizer *12*, the steam superheater *11* and enters the steam turbine mixing chamber *14* except the deaeration flow. In the mixer chamber, the steam is mixed with the high-pressure steam.

The high-pressure feed water is supplied to the economizer *10*, high-pressure vaporizer *9* and steam superheater *8* like in the low-pressure cir-cuit. The high-pressure steam enters the steam turbine *14* where it produces power. The turbine exhaust steam enters the condenser *16*.

The second version (Fig. 2b) shows an IGCC with pre-combustion cap-ture. This cycle arrangement differs from that in Fig. 2a. After the gasi-fication block, the syngas is preliminarily enriched in the water gas shift reactor *23*. Then in the physical absorption column *24*, it is cleaned from the carbon dioxide. The carbon dioxide is cooled in cooler *26*, compressed in compressor *22* and sent to the storage. From the enriched and cleaned syngas water is separated by condensing in the cooler *26* then it is supplied to the combustion chamber *5*.

(a) IGCC with post-combustion capture   (b) IGCC with pre-combustion capture

(c) oxy-fuel combustion power plant

Figure 2: Flow charts of highly efficient coal-fired TPP with low emissions.

The third unit (Fig. 2c) is a coal-fired oxy-fuel combustion power plant. Gasification block *3* is supplied with coal, oxygen and steam. The syngas is cooled in cooler *26* for a more efficient compression, then compressed in the fuel compressor *25* and supplied to the combustion chamber *5*. The syngas is fired in the almost pure oxygen produced by the ASU *1*. The combustion heat is transferred to the CO_2 flow passing the multi-flow regenerator *28*. Downstream of the combustion chamber *5* the working fluid is supplied to the carbon dioxide turbine *29* where it produces power. The turbine *29* exhaust flow enters the multi-flow regenerator *28* where it transfers its heat to the CO_2 flow, the turbine *29* coolant flow and the CO_2 with O_2 mixture flow. Also, the regenerator utilizes the low-potential heat of the ASU *1* outlet air flow. After regenerator *28*, its exhaust is supplied

to cooler-separator *30* where the working fluid water vapor is condensed.
Then the CO_2 flow is split into two flows, the main part is compressed in the multi-stage compressor *31* and the residual part is compressed in compressor *22* and stored.

After the multi-stage compressor *31*, the CO_2 flow is split into two equal parts. One of them is mixed with oxygen. After the carbon dioxide com-pressor *32*, the flow is again split into two parts. The smaller part works as the turbine *29* coolant and is heated in the regenerator *28*. In the regener-ator the main CO_2 flow with the CO_2 and O_2 mixture are also heated. The oxygen-carbon dioxide compressor *33* compresses the mixture up to the maximum temperature acceptable for the regenerator temperature drop. The hot flows that enter combustion chamber *5* from regenerator *28* re-duce the fuel flow needed for the working fluid heating up to the high temperature.

Table 2 presents the main parameters for modeling coal-fired power plants with coal gasification and CCS system. The fuel composition is taken according to [34]. The gas turbine inlet temperature of 1700◦C corresponds to the advanced developments [35]. The oxy-fuel combustion power cycle parameters are taken according to [20].

Table 2: Input data for TPP with coal gasification and low harmful emissions.

Parameter	Unit	Value
Fuel type	–	coal

Fuel composition:
    moisture (a.r.)
    ash
    carbon
    hydrogen
    nitrogen
    oxygen
    sulphur
    chlorine
	
	%
	%
	%
	%
	%
	%
	%
	%
		
		8.10
		14.19
		72.04
		4.08
		1.67
		7.36
		0.65
		0.01

Volatile matter (dry)	%	28.51
Oxygen purity	%	95.6
Gasifier pressure	MPa	3.5
Carbon storage pressure	MPa	10
Internal turbine/compressor/pump efficiency	%	89/88/85

Table 2 [cont.]

Parameter	Unit	Value
Mechanical, electric motor, power generator, heat transport efficiency	%	99
IGCC's/oxy-fuel combustion power plant's turbine inlet temperature	°C	1700/1100
Coolant flow rate of IGCC / oxy-fuel combustion power plant turbine	%	13.6/9.4
IGCC's/oxy-fuel combustion power plant's turbine inlet pressure	MPa	3/30
IGCC's/oxy-fuel combustion power plant's turbine outlet pressure	MPa	0.1013/3
High/low pressure of IGCC steam	MPa	8.55/0.7
Minimum temperature drop of IGCC high-/low-pressure heaters	°C	20/20
IGCC condenser pressure	kPa	4
Condensate temperature at the inlet to the condensate gas heater of the IGCC HRSG	°C	60
IGCC deaerator pressure	MPa	0.45
Minimum temperature drop of the multi-flow regenerator of the oxy-fuel combustion power plant	°C	5

3   Modeling approach

The thermodynamic analysis of TPP with coal gasification is carried out with the AspenONE Plus calculation models that consist of elements with the mass and energy transition between them. The elements models are the following:

- air separation unit that produces high purity oxygen, its modeling methodology is described in [36],

- gasification block with a steam-oxygen blast that transforms coal into syngas [37],

- combined cycle power unit producing electricity,

- oxy-fuel combustion power unit producing electricity,

- carbon capture and storage system.

The models of the IGCC with CCS system involves the following assump-tions:

- at the gas generator outlet the ash and syngas have equal tempera-tures;

- the syngas combustion in the combustion chamber is stoichiometric.

Figure 3 presents the mass and energy flow exchange between the main blocks of the mathematical model elements as the following:
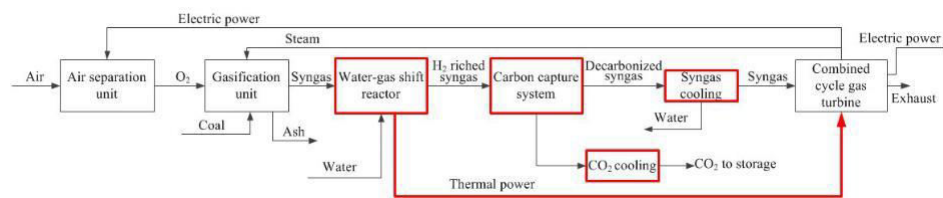
- IGCC with post-combustion carbon capture (Fig. 3a);

- IGCC with pre-combustion carbon capture (case 1), the heat produced in the fuel preliminary preparation system is not utilized (Fig. 3b);

- IGCC with pre-combustion carbon capture (case 2), the heat produced in the water gas shift reactor is utilized in the HRSG (Fig. 3c);

- IGCC with pre-combustion carbon capture (case 3), the heat produced in the water gas shift reactor and the syngas cooler is utilized in the HRSG (Fig. 3d);

- IGCC with pre-combustion carbon capture (case 4), the heat produced in the water gas shift reactor and the syngas and carbon dioxide coolers is utilized in the HRSG (Fig. 3e);

- coal-fired oxy-fuel combustion power plant (Fig. 3f).
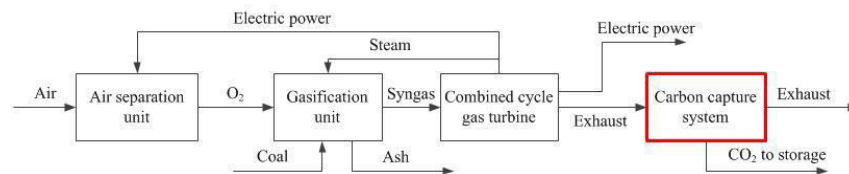
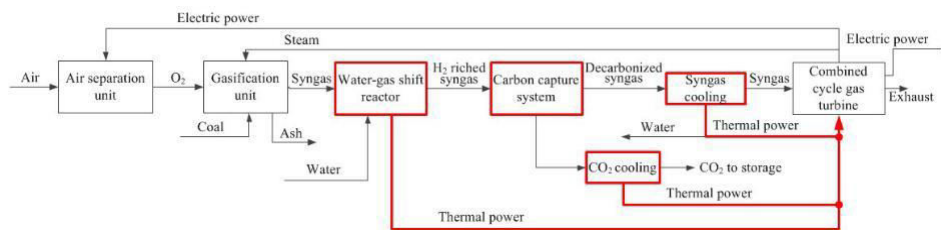(a) IGCC with post-combustion carbon capture
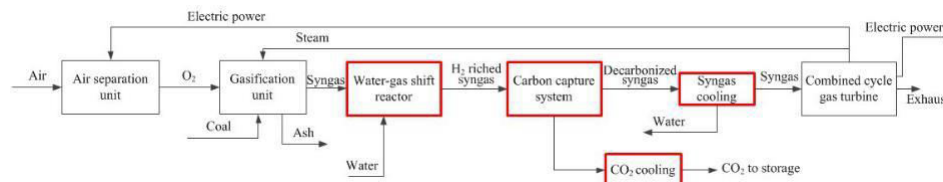
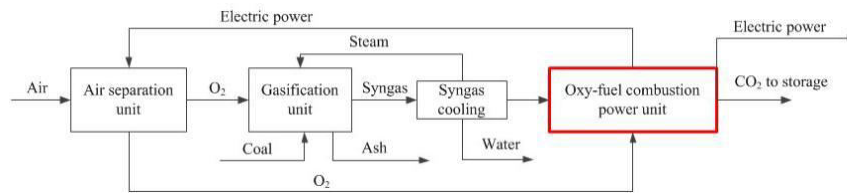(b) IGCC with pre-combustion carbon capture (case 1)

(c) IGCC with pre-combustion carbon capture (case 2)
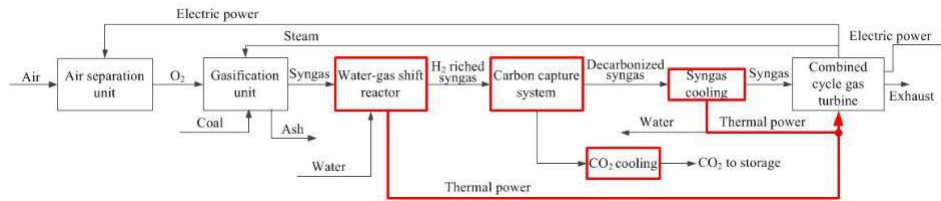
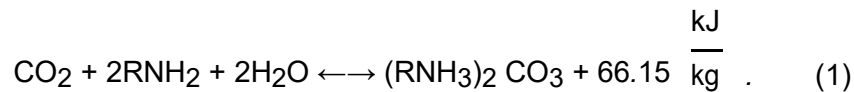(d) IGCC with pre-combustion carbon capture (case 3)

(e) IGCC with pre-combustion carbon capture (case 4)

(f) coal-fired oxy-fuel combustion power plant

Figure 3: Chart of the mathematical models of TPP with coal gasification and carbon capture systems.

The mathematical model of the dioxide carbon capture in the IGCC with post-combustion carbon capture by chemical absorption (Fig. 3a) involves two reactions. The first reaction between MEA and carbon dioxide is exo-thermal and passes at 40–60◦C

$$CO_2 + 2RNH_2 + 2H_2O \longleftrightarrow (RNH_3)_2 CO_3 + 66.15 \ \frac{kJ}{kg} \ . \qquad (1)$$

The second reaction is the endothermal desorption, absorbent regeneration reaction. The absorbed carbon dioxide is emitted at 110–120◦C

$$CO_2 + (RNH_3)_2 CO_3 + H_2O \longleftrightarrow 2RNH_3HCO_3 - 66.15 \ \frac{kJ}{kg} \ . \qquad (2)$$

Here the carbon dioxide capture degree is 90%.

In the analysis of the IGCC with pre-combustion carbon capture by physical absorption (Fig. 3b–3e), a process in water gas shift reactor described by the equation of the water gas shift exothermal reaction

$$CO + H_2O \longleftrightarrow CO_2 + H_2 + 41.2 \ \frac{kJ}{mol}. \qquad (3)$$
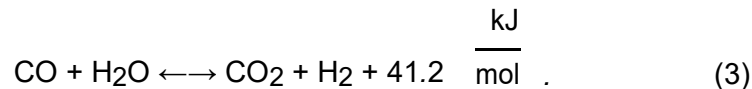
The next stage is the physical carbon dioxide absorption by the Selexol solvent from the hydrogen-enriched syngas. The Selexol is a mixture of various dimethyl ethers of polyethylene glycol $CH_3O(C2H_4O)_nCH_3$, where n is in the range from 2 to 9. The degree of carbon dioxide capture with the Selexol solvent is 95% [38]. Then the syngas is cooled to condense the ballast water vapor and the carbon dioxide is cooled for more efficient compression in the compressor.

The simulation models allowed the investigation of advanced coal-fired TPP with different carbon dioxide capture systems.

4 Modeling results

At the first stage, the analysis was carried out for the IGCC without carbon dioxide capture. This power plant's net efficiency is 53.5% and the carbon dioxide emission is 817 gm/kWh, while combined cycle power plants fired with natural gas without carbon capture have a net efficiency equal to 63.5% according to [39]. The rather low coal-fired power plant efficiency is due to the remarkable losses of 5.8% in the gasification block and the high auxiliary electricity requires for the oxygen production by ASU of 5.9% and its compression upstream the combustion chamber of 1.9%. The high CO_2 emissions for the IGCC are due to the high carbon content. Coal fuel has a 20% higher carbon content compared to natural gas fuel, where emissions are below 450 g/kWh.

At the next stage of the thermodynamic analysis, the effect of carbon capture and storage system on the IGCC energy and environmentally safe performances was estimated. The post-combustion CO_2 capture allows the carbon dioxide emission reduction down to 90 g/kWh. In this version, the TPP net efficiency is as low as 46.6%. The lower efficiency of the coal-fired TPP compared to the IGCC without CO_2 capture is due to the power losses for CO_2 capture. In turn, the natural gas combined cycle power plants with post-combustion CO_2 capture are more efficient compared to the IGCC with post-combustion CO_2 capture due to the lack of gasifica-

tion. According to the research [39], the net efficiency of these plants could achieve 56.9%.

The results of the thermodynamic analysis of the IGCC with pre-combustion carbon capture (case 1) show that the efficiency of this power plant without the utilization of the heat produced in the fuel preparation is 42.3%. Utilization of the water gas shift reactor heat allows higher efficiency of 45.2% (case 2). Utilization of the reactor and the syngas cooler heat (case 3) flows results in the efficiency increase up to 46.5% and utilization of the reactor syngas' and carbon dioxide coolers' thermal power up to 47.2% (case 4). The last case has the carbon dioxide emission of 103 g/kWh, which is 13 g/kWh higher than in the carbon dioxide capture from the exhaust gas. This is due to the large syngas consumption with its binding and the further separation from it of the combustible carbon monoxide.

Part of the heat produced in the fuel preparation in the TPP with pre-combustion capture heat balance is remarkably large so its utilization considerably influences the TPP efficiency improvement. For example, the thermal power emitted in the reactor and coolers is about 23% of the coal combustion heat power. Utilization of this heat in the HRSG reduces the concerned losses to 5% (Fig. 4). The HRSG thermal power increase allows the 5% steam turbine power increase and its condenser heat losses become

1. Exhaust losses
2. Condensation losses
3. Thermal power losses in shift gas water reactor and coolers of syngas and CO2
4. Thermal power losses in compressor coolers
5. Gasigication losses
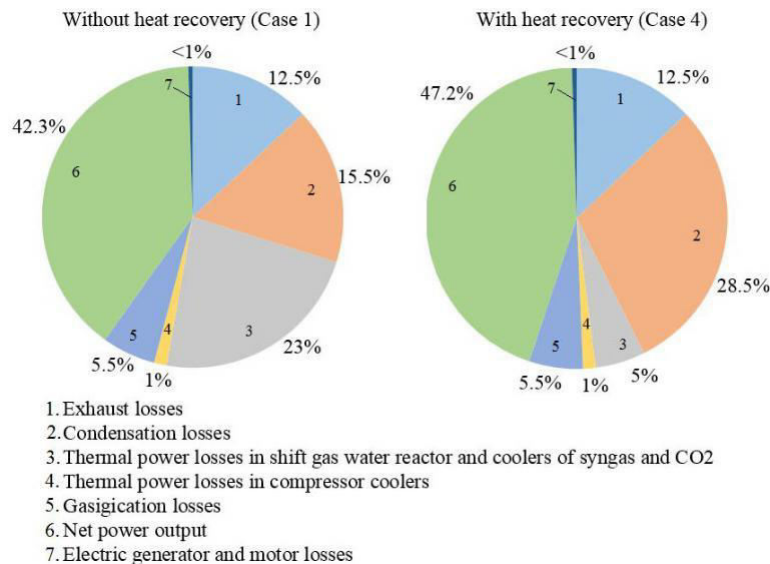6. Net power output
7. Electric generator and motor losses

Figure 4: Heat balance of IGCC with pre-combustion carbon capture without heat recovery (case 1) and with heat recovery (case 4).

by 13% smaller. Thus, the utilization of the fuel preparation heat increases the cycle net efficiency by almost 5%.

The coal gasification oxy-fuel combustion power cycle has a net efficiency of 36.3% which is the lowest among the low emission power production cycles. This low thermal efficiency is mostly due to the turbine inlet parameters lower than those of the combined cycle. Syngas must be cooled before its compression and supplied to the combustion chamber, but about 10.9% of the cycle consumed power is lost in the syngas cooling after the gasification block. Moreover, the oxygen production by ASU and its compression before combustion consume about 19% of the turbine power production (Fig. 5), which also reduces the net efficiency by the larger TPP auxiliary electricity requirements. The net efficiency of the natural gas-fired oxy-fuel combustion power plants is almost 11% higher according to the modeling results presented in [40] due to zero energy consumption for gasification.
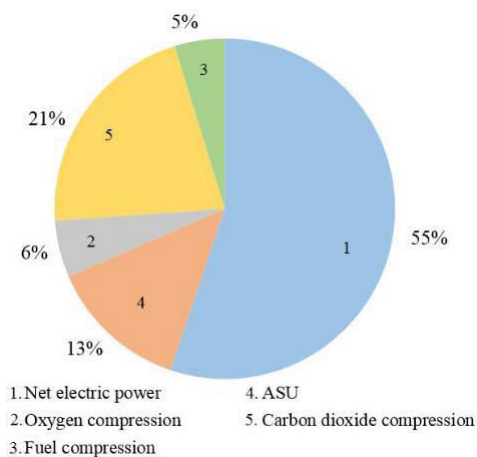

Figure 5: The distribution of power generated by the turbine of the oxy-fuel combustion power plant.

Figures 6, 7, and 8 demonstrate evaluation of thermal efficiency and environmental safety of the reviewed above advanced TPPs with coal gasification and carbon capture and storage systems. The maximal efficiency of 47.2% is reached in a coal-fired combined cycle TPP with the carbon dioxide capture from syngas and utilization of the heat produced in the syngas preparation. In the case of CO_2 capture from exhaust gases, the net efficiency is 46.6%. The coal-fired oxy-fuel combustion power cycle has the

smallest efficiency of 36.3%. In turn, the oxy-fuel combustion power plant has a minimum carbon dioxide emission of 9 g/kWh.

Table 3 summarizes the thermal efficiency and environmental safety performance in different coal- and natural gas-fired TPPs. The coal- and natural gas-fired combined cycle power plants have the highest thermal efficiency. On the other side, the oxy-fuel combustion power plant has the best environmental safety with carbon dioxide emissions below 10 g/kWh.

Table 3: Energy and environmental indicators of various types TPPs.

TPP type	Initial temperature, $^\circ$C	Natural gas		Coal		
		Net efficiency, %	Specific CO_2 emissions, g/kWh	Net efficiency, %	Specific CO_2 emissions, g/kWh	SPECCA (coal-fired TPP), MJ/kg$_{CO_2}$
Steam turbine plant						
with carbon capture (post-combustion capture)	600–650	47.0	500	44.5	983	–
with carbon capture (post-combustion capture)		41.3	50	38.5	98	1.42
Combined cycle power plant						
without carbon capture	1600–1700	63.5	374	53.5	817	–
with carbon capture						
post-combustion capture		56.9	37	46.6	90	1.37
pre-combustion capture (case 1)		–	–	42.3	115	2.52
pre-combustion capture (case 4)		–	–	47.2	103	1.26
Oxy-fuel combustion power plant						
with carbon capture (oxy-combustion capture)	1100	47.0	4.19	36.3	9	–

A measure of the energy cost related to CO_2 capture was estimated by the specific primary energy consumption for CO_2 avoided (SPECCA), which is defined as in [41]. According to the research [41], SPECCA for the IGCC with pre-combustion carbon capture is 3.71 MJ/kg$_{CO_2}$. In this paper,

1. Exhaust losses
2. Cooling looses
3. Net power output
4. Syngas cooling losses
5. Condensation losses
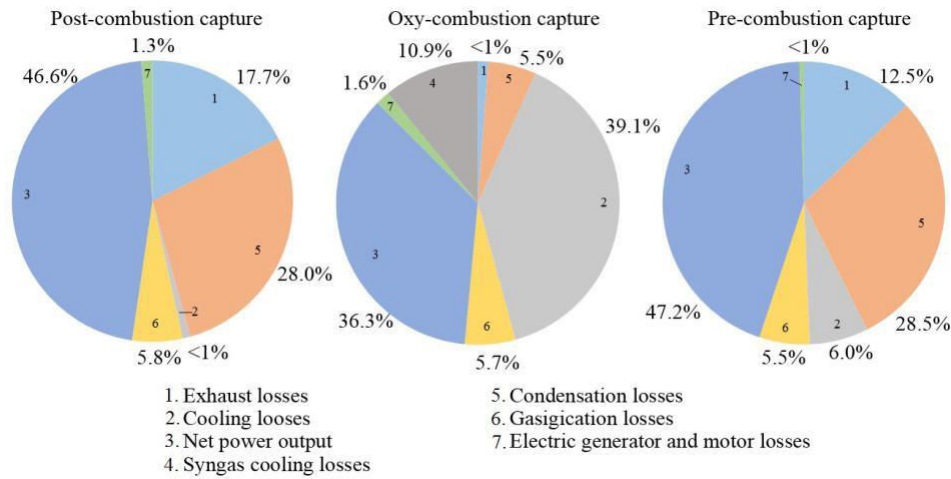6. Gasigication losses
7. Electric generator and motor losses

Figure 6: The distribution of thermal power supplied to the TPPs with coal gasification and CCS system.
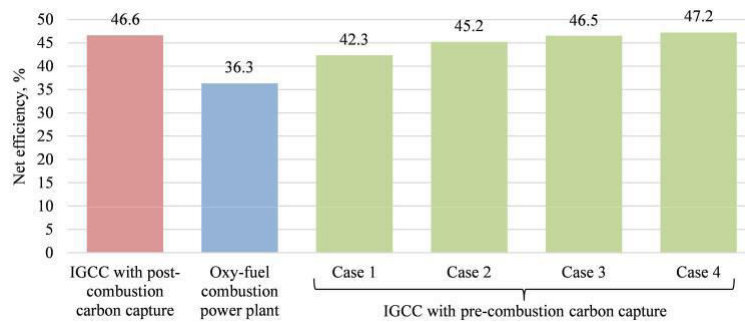

Figure 7: Net efficiency of TPP with coal gasification and low harmful emissions.
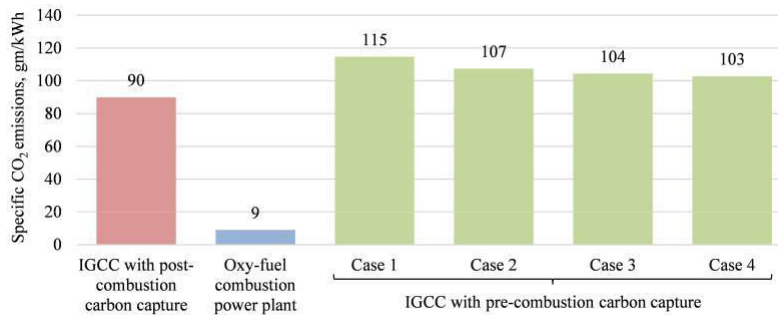

Figure 8: Specific CO_2 emissions of TPP with coal gasification and low harmful emissions.

SPECCA is 2.52 MJ/kg$_{CO2}$ for IGCC with pre-combustion carbon capture (case 1), but for the IGCC with pre-combustion carbon capture (case 4), it is equal to 1.26 MJ/kg$_{CO2}$. Such a low energy consumption for CO_2 removal and high SPECCA value can be explained by the presence of regeneration in case 4 and higher value of initial temperature, which in itself leads to an increase in net efficiency of a power plant.

5   Conclusions

The mathematical simulation models for the TPP with coal gasification and carbon capture and storage systems allowed assessment of the TPP with pre- and post-combustion capture and oxy-fuel combustion power and financial performance, were developed.

The thermal efficiency of the integrated gasification combined cycle with pre-combustion CO_2 capture is 47.2% which is 0.6% higher than the post-combustion one and 9.9% higher than the oxy-fuel combustion. The pre-combustion capture net efficiency is remarkably influenced by the utiliza-tion of the heat produced by the water gas shift reactor and the capture system coolers which is about 23% of the cycle thermal power.

The carbon capture and storage system in a combined cycle TPP with coal gasification may reduce harmful emissions from 817 to below 110 g/kWh and application of the oxy-fuel combustion power cycles to below 10 g/kWh.

The combined cycle TPP with coal gasification and carbon dioxide cap-ture and storage systems have higher power production efficiency of 46.6– 47.2% than the 38.5% in the coal-fired supercritical steam turbine TPP equipped with CCS which is due to the higher mean-integral heat supply temperature in the combined cycle.

References

[1] Friedlingstein P., O'Sullivan M., Jones M.W., Andrew R.M., Hauck J., Olsen A., Zaehle S.: *Global carbon budget 2020*. Earth Syst. Sci. Data **12**(2020), 4, 3269–3340.

[2] Peters G.P., Andrew R.M., Canadell J.G., Friedlingstein P., Jack-son R.B., Korsbakken J.I., Peregon A.: *Carbon dioxide emissions continue to grow amidst slowly emerging climate policies*. Nat. Clim. Change **10**(2020), 1, 3–6.

[3] Le Quéré C., Korsbakken J.I., Wilson C., Tosun J., Andrew R., An-dres R.J., van Vuuren D.P.: *Drivers of declining CO_2 emissions in 18 developed economies*. Nat. Clim. Change **9**(2019), 3, 213–217.

[4] Bui M., Adjiman C.S., Bardow A., Anthony E.J., Boston A., Brown S., Mac Dowell N.: *Carbon capture and storage (CCS): The way forward*. Energ. Environ. Sci. **11**(2018), 5, 1062–1176.

[5] Tong D., Zhang Q., Zheng Y., Caldeira K., Shearer C., Hong C., Qin Y., Davis S.J.: *Committed emissions from existing energy infrastructure jeopardize 1.5°C climate target*. Nature **572**(2019), 7769, 373–377.

[6] Nejat P., Jomehzadeh F., Taheri M.M., Gohari M., Majid M.Z.A.: *A global review of energy consumption, CO_2 emissions and policy in the residential sector (with an overview of the top ten CO_2 emitting countries)*. Renew. Sust. Energ. Rev. **43**(2015), 843–862.

[7] Vega F., Baena-Moreno F.M., Fernández L.M.G., Portillo E., Navarrete B., Zhang Z.: *Current status of CO_2 chemical absorption research applied to CCS: Towards full deployment at industrial scale*. Appl. Energ. **260**(2020), 114313.

[8] Fan J.L., Xu M., Li F., Yang L., Zhang X.: *Carbon capture and storage (CCS) retrofit potential of coal-fired power plants in China: The technology lock-in and cost optimization perspective*. Appl. Energ. **229**(2018), 326–334.

[9] Porter R.T., Fairweather M., Kolster C., Mac Dowell N., Shah N., Wool-ley R.M.: *Cost and performance of some carbon capture technology options for pro-ducing different quality CO_2 product streams*. Int. J. Greenh. Gas Con. **57**(2017), 185–195.

[10] Erlach B., Schmidt M., Tsatsaronis G.: *Comparison of carbon capture IGCC with pre-combustion decarbonisation and with chemical-looping combustion*. Energy **36**(2011), 6, 3804–3815.

[11] Atsonios K., Koumanakos A., Panopoulos K.D., Doukelis A., Kakaras E.: *Techno-economic comparison of CO_2 capture technologies employed with natural gas derived GTCC*. In: Proc. ASME Turbo Expo: Turbine Tech. Conf. Exp, San Antonio, June 3–7, 2013, GT2013-95117, V002T07A018.

[12] Kanniche M., Gros-Bonnivard R., Jaud P., Valle-Marcos J., Amann J.M., Bouallou C.: *Pre-combustion, post-combustion and oxy-combustion in thermal power plant for CO_2 capture*. Appl. Therm. Eng. **30**(2010), 1, 53–62.

[13] Merkel T.C., Lin H., Wei X., Baker R.: *Power plant post-combustion carbon dioxide capture: An opportunity for membranes*. J. Membrane Sci. **359**(2010), 126–139.

[14] Merkel T.C., Zhou M., Baker R.W.: *Carbon dioxide capture with membranes at an IGCC power plant*. J. Membrane Sci. **389**(2012), 441–450.

[15] Merkel T.C., Wei X., He Z., White L.S., Wijmans J.G., Baker R.W.: *Selec-tive exhaust gas recycle with membranes for CO_2 capture from natural gas combined cycle power plants*. Ind. Eng. Chem. Res. **52**(2013), 3, 1150–1159.

[16] Song C., Liu Q., Deng S., Li H., Kitamura Y.: *Cryogenic-based CO_2 capture technologies: state-of-the-art developments and current challenges*. Renew. Sust. En-erg. Rev. **101**(2019), 265–278.

[17] Chiesa P., Campanari S., Manzolini G.: *CO_2 cryogenic separation from com-bined cycles integrated with molten carbonate fuel cells*. Int. J. Hydrogen Energ. **36**(2011), 16, 10355–10365.

[18] Komarov I., Kharlamova D., Makhmutov B., Shabalova S., Kaplanovich I.: *Natural gas-oxygen combustion in a super-critical carbon dioxide gas turbine com-bustor*. E3S Web Conf. **178**(2020), 01027.

[19] Allam, R., Martin, S., Forrest, B., Fetvedt, J., Lu, X., Freed, D., Brown Jr. G.W., Sasaki T., Itoh M., Manning J.: *Demonstration of the Allam cycle: An update on the development status of a high efficiency supercritical carbon dioxide power process employing full carbon capture*. Enrgy Proced. **114**(2017), 5948–5966.

[20] Rogalev A., Kindra V., Osipov S., Rogalev N.: *Thermodynamic analysis of the net power oxy-combustion cycle*. In: Proc. 13th Eur. Conf. on Turbomachinery Fluid Dynamics and Thermodynamics, ETC13, Lausanne, April 8-12, 2018, ETC2019-030.

[21] Mukherjee S., Kumar P., Yang A., Fennell P.: *Energy and exergy analysis of chemical looping combustion technology and comparison with pre-combustion and oxy-fuel combustion technologies for CO_2 capture*. J. Environ. Chem. Eng. **3**(2015), 3, 2104–2114.

[22] Li J., Zhang H., Gao Z., Fu J., Ao W., Dai J.: *CO_2 capture with chemical looping combustion of gaseous fuels: An overview*. Energ. Fuels **31**(2017), 4, 3475–3524.

[23] Lyngfelt A., Linderholm C.: *Chemical-looping combustion of solid fuels–status and recent progress*. Enrgy Proced. **114**(2017), 371–386.

[24] Naqvi R., Bolland O.: *Multi-stage chemical looping combustion (CLC) for com-bined cycles with CO_2 capture*. Int. J. Greenh. Gas Con. **1**(2007), 1, 19–30.

[25] Li K., Leigh W., Feron P., Yu H., Tade M.: *Systematic study of aqueous mo-noethanolamine (MEA)-based CO_2 capture process: Techno-economic assessment of the MEA process and its improvements*. Appl. Energ. **165**(2016), 648–659.

[26] Duan L., Zhao M., Yang Y.: *Integration and optimization study on the coal-fired power plant with CO_2 capture using MEA*. Energy **45**(2012), 1, 107–116.

[27] Ma Y., Gao J., Wang Y., Hu J., Cui P.: *Ionic liquid-based CO_2 capture in power plants for low carbon emissions*. Int. J. Greenh. Gas Con. **75**(2018), 134–139.

[28] Oh S.Y., Binns M., Cho H., Kim J.K.: *Energy minimization of MEA-based CO_2 capture process*. Appl. Energ. **169**(2016), 353–362.

[29] Ho M.T., Allinson G.W., Wiley D.E.: *Comparison of MEA capture cost for low CO_2 emissions sources in Australia*. Int. J. Greenh. Gas Con. **5**(2011), 1, 49–60.

[30] Rogalev A., Kindra V., Osipov S.: *Modeling methods for oxy-fuel combustion cycles with multicomponent working fluid*. AIP Conf. Proc. **2047**(2018), 1, 020020.

[31] Kunze C., Spliethoff H.: *Assessment of oxy-fuel, pre-and post-combustion-based carbon capture for future IGCC plants*. Appl. Energ. **94**(2012), 109–116.

[32] Scaccabarozzi R., Gatti M., Martelli E.: *Thermodynamic analysis and numer-ical optimization of the NET Power oxy-combustion cycle*. Appl. Energ. **178**(2016), 505–526.

[33] Rogalev A.N., Kindra V.O., Rogalev N.D., Sokolov V.P., Milukov I.A.: *Methods for efficiency improvement of the semi-closed oxy-fuel combustion combined cycle*. J. Phys. Conf. Ser. **1111**(2018), 1, 012003.

[34] Cormos C.-Cr.: *Integrated assessment of IGCC power generation technology with carbon capture and storage (CCS)*. Energy **42**(2012), 434–445.

[35] Ito E., Okada I., Tsukagoshi K., Muyama A., Masada J.: *Development of key technologies for the next generation 1700C-class gas turbine*. In: Proc. ASME Turbo Expo 2009: Power for Land, Sea, and Air, Orlando, June 8–12, 2009. 919–929.

[36] Ebrahimi A., Meratizaman M., Reyhani H.A., Pourali O., Amidpour M.: *En-ergetic, exergetic and economic assessment of oxygen production from two columns cryogenic air separation unit*. Energy **90**(2015), 1298–1316.

[37] Uddin F., Taqvi S.A., Memon I.: *Process simulation and sensitivity analysis of indirect coal gasification using Aspen Plus model*. J. Eng. Appl. Sci. **11**(2016), 17, 10546–10552.

[38] Kapetaki Z., Brandani P., Brandani S., Ahn H.: *Process simulation of a dual-stage Selexol process for 95% carbon capture efficiency at an integrated gasification combined cycle power plant*. Int. J. Greenh. Gas Con. **39**(2015), 17–26.

[39] Kotowicz J., Brzęczek M.: *Comprehensive multivariable analysis of the possibil-ity of an increase in the electrical efficiency of a modern combined cycle power plant with and without a CO_2 capture and compression installations study*. Energy **175** (2019), 1100–1120.

[40] Kvamsdal H.M., Jordal K., Bolland O.: *A quantitative comparison of gas tur-bine cycles with CO_2 capture*. Energy **175**(2007), 10–24.

[41] Gazzani M., Macchi E., Manzolini G.: *CO_2 capture in integrated gasifica-tion combined cycle with SEWGS – Part A: Thermodynamic performances*. Fuel **105**(2013), 206–219.